International Scientific Journal
Environmental Science
http://environment.scientific-journal.com

Heat Transfer Enhancement in a Channel with New Longitudinal Vortex Generators

Sinan Caliskan
Department of Mechanical Engineering
Hitit University
Corum,Turkey
sbycaliskan@gmail.com

Mehmet Eren
Department of Mechanical Engineering
Hitit University
Corum,Turkey
mehmeteren@hitit.edu.tr

***Abstract*— In plate-fin or fin-tube heat exchangers the flow between the plates can be considered as a channel flow. For reduction of the thermal resistance, the heat transfer coefficient needs to be augmented. The heat transfer coefficient can be increased by longitudinal vortex generators (LVGs), which can be punched from the main plates or attached to them. In this study, the augmentations of heat transfer in a rectangular channel with triangular and rectangular vortex generators are evaluated. A longitudinal vortex generators (LVGs) on heat transfer surface is one of the most widely employed heat transfer enhancement techniques. This technique is used for thermal equipment such as heat exchanger, internal and blade cooling of gas turbine. A new punched triangular vortex generators (PTVGs) and punched rectangular vortex generators (PRVGs) are developed. The triangular and rectangular vortex generators were punched directly from the longitudinal winglet at attack angles of, 15º, 45º, and 75º, respectively. Measurements are carried out for a rectangular channel of aspect ratio AR=2, winglet transverse pitch (S) to longitudinal winglet height (e) ratio of S/e=0.59, and a winglet height (e) to channel height (H) ratio of e/H= 0.8. The Reynolds numbers considered for the channel flow case. The heat transfer results were obtained using an infrared thermal imaging technique. The heat transfer results of the vortex generators are compared with those of a smooth plate. Also pressure drop results are compared with those of smooth plate. The best heat transfer performance was obtained with the PTVGs.**

Keywords*— *Punched vortex generators; Heat transfer enhancement; Infrared camera; Pressure drop

I. INTRODUCTION

The need of high-performance thermal systems in engineering applications has simulated interest in finding ways to augmentation heat transfer rate in the system. A longitudinal vortex generators (LVGs) on a heat transfer surface is one of the most widely employed heat transfer enhancement techniques. This technique is used for thermal equipment such as a heat exchanger and the internal blade cooling of gas turbine. Comprehensive studies have conducted to increase using turbulators in simulated heat exchangers, turbine blades and etc. [1-6].

Tigglebeck et al. [1] found in a rectangular channel flow that a pair of delta winglets perform slightly better heat transfer than a pair of rectangular winglets at higher attack angles and Reynolds numbers. Biswas et al. [2] reported that a winglet pair have less loss of flow than that of a single winglet. Their study also suggested that and winglets pair can eliminate the poor heat transfer zones.

Fiebig et al. [3] studied the heat transfer enhancement of four different kinds of LVGs (delta wing, delta winglet pair, rectangular wing and rectangular winglet pair) in flat plate laminar rectangular channel flow. The Reynolds numbers in that study were taken as between 1360 and 2270.

Gentry and Jacobi [4, 5] experimentally studied the heat transfer enhancement characteristic of delta wing vortex generators in a flat-plate channel flow by using a naphthalene sublimation technique. Their experiments showed that the average heat transfer could be enhanced by 50-60% at a low Reynolds number in comparison with the original configuration.

Zhou and Ye [6], in a joint experiment, investigated the heat transfer performance of a new vortex generator called curved trapezoidal winglet and compared the results with the rectangular winglets.

In this study, new longitudinal vortex generators (LVGs) have been designed. An experimental set-up was established in order to investigate the convective heat transfer performance of LVGs. The effects of the attack angle of LVGs on the heat transfer enhancement are examined.

II. EXPERIMENTAL SETUP

As shown in Fig. 1, the heat transfer experiments are conducted in an open rectangular channel. It consist of an entrance section, a test section, a centrifugal blower, an infrared thermography system, vortex generators, and devices for measuring flow velocity, temperature and pressure difference. Air was drawn in by a variable speed fan and passed through the test section of the channel. The rectangular channel has inner cross section dimensions of 100mm x 50mm. Length of the entrance channel is 2500mm. The channel was constructed from plexiglass plates of 9mm thickness. The dimensions of the heating plate were 100mm (width) x 270mm (length). In the experiments, the heating plate was made of stainless steel foil. It was firmly clamped and stretched between two copper bus bars. The foil was

electrically heated by means of a high current DC power supply to provide a constantly heated flux surface. The longitudinal winglets were mounted on the bottom of the channel to enhance the convective transfer of heat transfer. The averaged heat transfer coefficient on the surface of the plate was measured for various rates of airflow through the channel.

Views of both the PTVGs and PRVGs are shown in Fig. 2. The longitudinal winglets were made of high conductivity aluminum material. The longitudinal winglets were attached to the stainless steel foil plates by a thin layer of super-glue. The thermal contact resistance due to the super-glue introduced a minor conservative preference to the reported results [7]. Thermal images were obtained from an IR camera positioned on the bottom of the heater assembly vertical to the channel. The Kimo LV107-type anemometer connected to the output of the blower are used for the air velocity measurement. For the pressure drop determine ALMEMO and a pressure transducer are used at between the air inlet and outlet at the test section. The inlet and outlet temperatures of the channel air were measured in different locations of the channel by using a K-type thermocouple. All of these thermocouples were connected to a PC-based data acquisition system. The infrared thermography system, which included a ThermaCAM SC500 camera from FLIR systems and a PC with AGEMA Researcher software, could measure temperatures from -20 ºC to 1200 ºC with an accuracy of ±2%. The infrared camera used an uncooled focal plane array detector with 320x240 pixels, which operated over a wavelength range of 7.5-13. The field of view was 25ºx18.8º/0.4m; the instantaneous field of view was 1.3 m-rad, and the thermal sensitivity was 0.07 ºC at 30 ºC. The images captured by the infrared camera were displayed and recorded using a computer for further analysis.

.

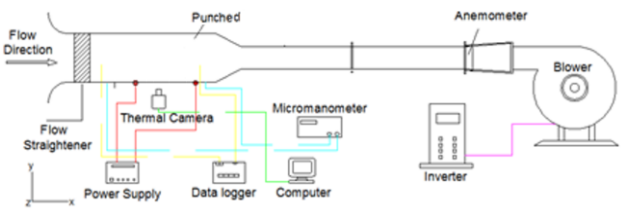

Fig. 1. Experimental set-up

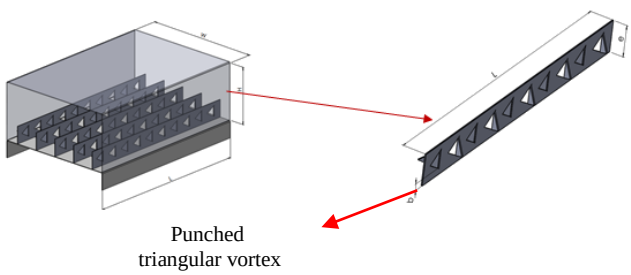

(a)

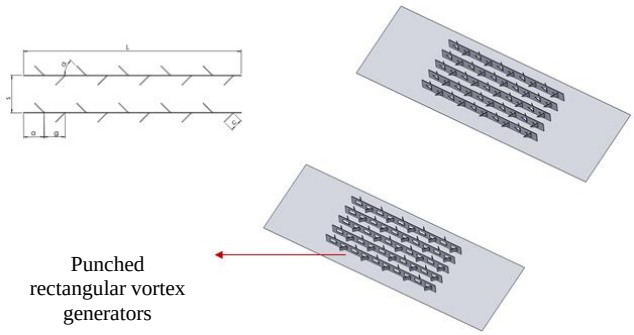

(b)

Fig. 2. Schematic view of present vortex generators

The bottom side of the stainless steel foil was covered with a layer of black backing paint. The emissivity of each side of the plate was measured with an AE anemometer and was found to be 0.82 and 0.13 for the painted and unpainted surfaces, respectively.

The local heat transfer coefficient and Nusselt number were defined as:

$$h_x = \frac{q_{conv}}{(T - T_{b,x})} \tag{1}$$

where T and T_{bx} were the local temperature of the heating surface and the bulk fluid, respectively.

$$Nu_x = \frac{h_x D_h}{k} \tag{2}$$

The convective heat flux was evaluated as follows:

$$q_{conv} = \frac{Q_{el} - Q_{loss}}{A} \tag{3}$$

where Q_{el} was the measured input power to the heater. Radiation, free convection from the bottom side, and conduction were considered heat losses. The radiation heat flux from both sides of the sheet was given by

$$q_r^{\ front} = \varepsilon_t \sigma \left(T^4 - T_b^4 \right) \tag{4}$$

$$q_r^{\ back} = \varepsilon_b \sigma \left(T^4 - T_\infty^4 \right) \tag{5}$$

where ε_t and ε_b are the emissivities of the painted and unpainted surfaces, respectively. For the symbol σ, it is the Stefan-Boltzmann constant.

The free convection heat flux from the bottom side of the sheet was calculated using

$$q_f = h_f \left(T - T_\infty \right) \tag{6}$$

where the free convection coefficient h_f was defined as 1.1 W/m^{2}K, for an air velocity of 0.1 m/s [8].

The conduction was given by:

$$q_c = k\frac{\Delta T}{t} \tag{7}$$

where k was the thermal conductivity of the sheet, ΔT was the temperature difference across the sheet, and t was the thickness of the sheet. As a result of the thinness of the sheet, the lateral conduction was negligible as reported by Lytle and Webb [9]. The sum of Q_{loss} was typically in the range of 7.4 to 10.6% of Q_{el} at the highest Reynolds number.

The averaged Nusselt number Nu_{ave} was calculated by integrating the local Nusselt number over the heating surface, i.e.,

$$Nu_{ave} = \frac{1}{L}\int Nu(x)\partial x \tag{8}$$

The Reynolds number based on the channel hydraulic diameter was given by

$$\mathrm{Re} = \frac{\rho u D_h}{\mu} \tag{9}$$

where D_h=2WH/(W+H) was the channel hydraulic diameter.

Friction factor, f, can be written as

$$f = \frac{\Delta P}{\left(\frac{L}{D_h}\right)\rho u^2/2} \tag{10}$$

where Δp was the drop in pressure across the length of the channel, L.

Here, the experimental uncertainty components are evaluated with a standard error analysis. Both the inlet and outlet temperatures of the air were measured by using calibrated K-type thermocouples with an accuracy of 0.3 °C. The inlet velocities at the center of both thermocouples were measured by an anemometer with 0.03 m/s of uncertainty. The uncertainty in the experimental data was determined according to the procedure proposed by Kline and McClintock [10]. In our experiment, the fluid properties were assumed constant. The resulting uncertainty for the Reynolds number and Nusselt number was calculated to be below 6.7% and 5.8%, respectively. The uncertainty in the Nusselt number was estimated to be 4.2% at the highest Reynolds number and 6.7% at the lowest Reynolds numbers. The maximum uncertainty of the infrared thermography measurements was less than ±1.5%.

III. RESULTS AND DISCUSSION

The experimental data for the forced convection heat transfer and friction factor in a rectangular duct for the both PTVGs and PRVGs was examined. The present experimental results in a smooth channel were first validated with the Nusselt number and the friction factor. The Nusselt number and the friction factor obtained from the present smooth channel were, respectively, compared with the correlations of Dittus-Boelter and Blasius found in the open literature [11] for turbulent flow in ducts.

Correlation of Dittus-Boelter,

$$Nu = 0.023\mathrm{Re}^{0.8}\,\mathrm{Pr}^{0.4} \text{ for heating} \tag{11}$$

Correlation of Blasius,

$$f = 0.316\mathrm{Re}^{-0.25} \text{ for } 3000 \le \mathrm{Re} \le 20{,}000 \tag{12}$$

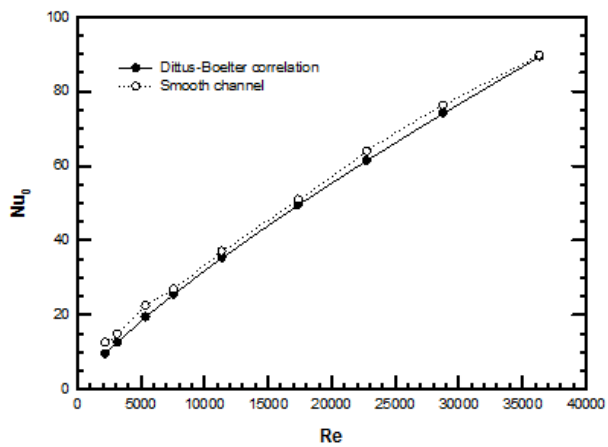

Fig. 3. Verification of Nusselt number for smooth channel

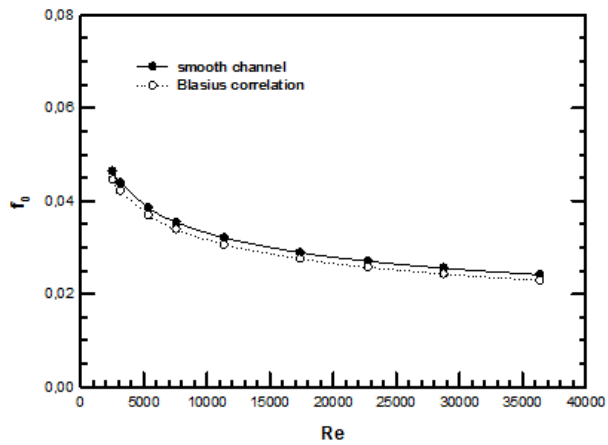

Fig. 4. Verification of friction factor for smooth channel

Fig. 3 and 4 shows, respectively, a comparison of the Nusselt number and the friction factor obtained from the present work with those from correlations of Eqs. (11) and (12). In the figures, the present results reasonably agree well within the ±11.8% deviation for both the friction factor and Nusselt number correlations.

A. Effect of attack angle and vortex geometry

The Nusselt numbers obtained under turbulent flow conditions for both PTVGs and PRVGs, with b/e=0.05 distance of punched winglet from the channel bottom and different attack angle, are presented in Fig. 5. As shown in Fig. 5, the use of vortex generators (PTVGs and PRVGs) leads to a considerable heat transfer enhancements in a trend similar to and in comparison with the smooth channel and the Nusselt number values, and increase with the rise of the Reynolds number. The maximum average Nusselt numbers were obtained at Re=36362 for PTVGs. The maximum difference in the averaged Nusselt number between smooth and PTVGs plates is found to occur at, and Re=37817.

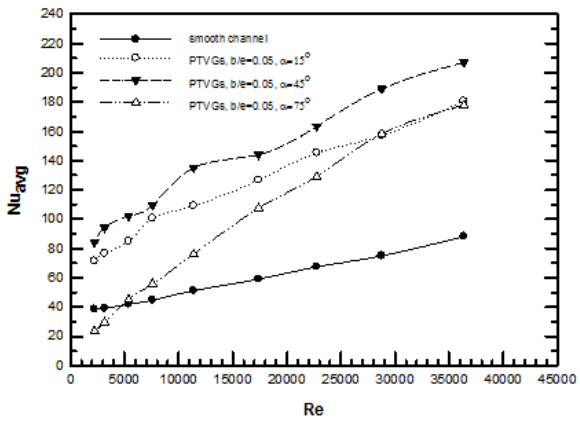

(a)

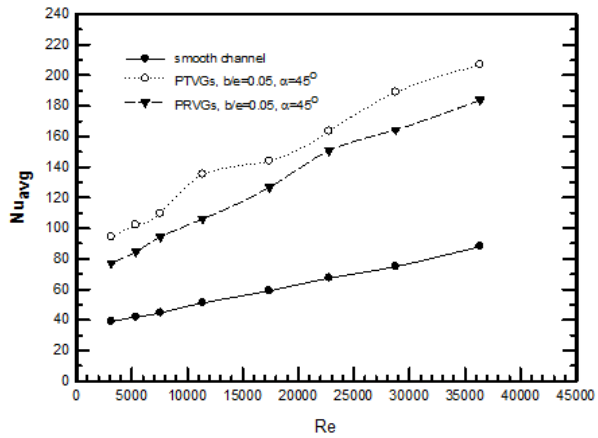

(b)

Fig. 5. Nusselt number for varying Reynolds number and α=45°

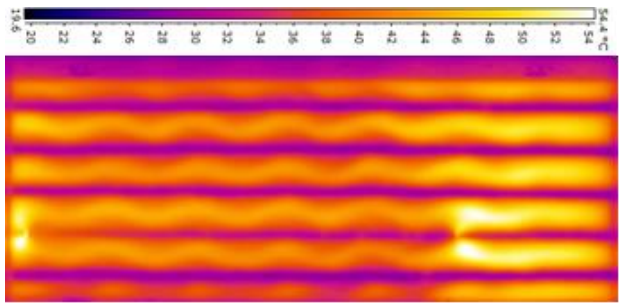

(a) Re=5375 PTVGs (b/e=0.05, α=45°)

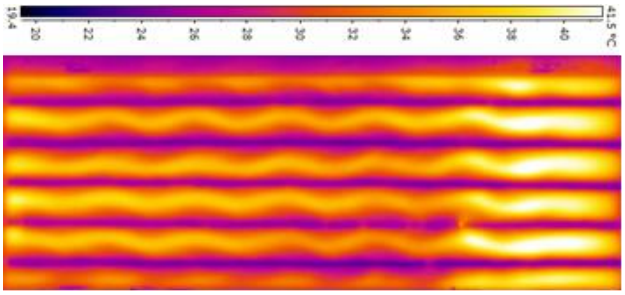

(b) Re=17390 PTVGs (b/e=0.05, α=45°)

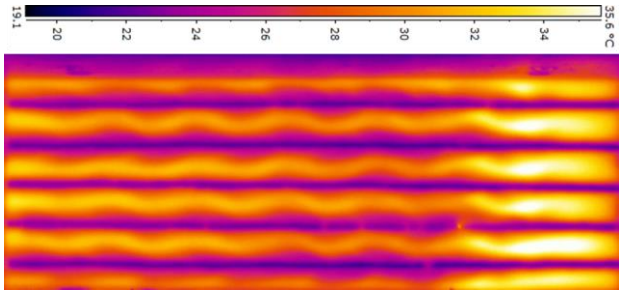

(c) Re=36362 PTVGs (b/e=0.05, α=45°)

(d) Re=36362 smooth surface

Fig. 6. Temperature contours for the PTVGs for α=45o and smooth surface

Fig. 6a, b and c present the temperature contours for the PTVGs in both the streamwise and the spanwise directions for the different Reynolds number. As shown in Fig. 6a, b and c, the temperature is decreases with increasing of the Reynolds number. The wall temperatures for 45° vortex generator angle and b/e=0.05 PTVGs surface were lower than the smooth surface, which disrupted the boundary layer more, resulting in a better heat transfer.

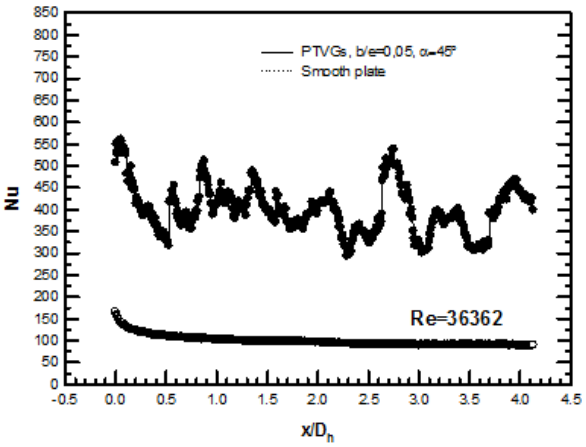

(a)

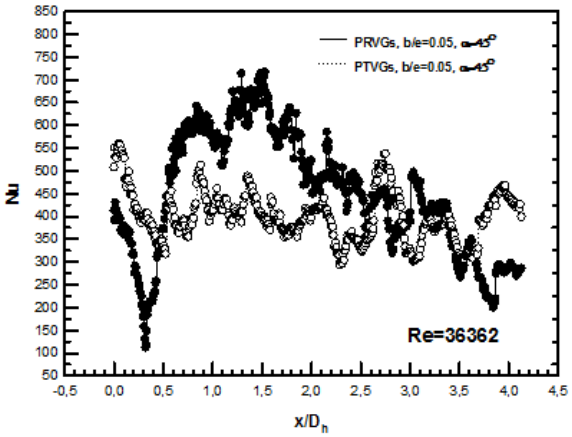

(b)

Fig. 7. Local Nusselt number distribution for b/e=0.05 and α=45°

The local Nusselt number distributions were presented in Fig. 7. As shown in Fig. 7, the local Nusselt number of the PRVGs was higher than for the smooth channel and PTVGs.

IV. CONCLUSIONS

An experimental investigation in a rectangular duct with PTVGs and PRVGs under uniform heat flux conditions has been performed.

The following conclusions have been drawn:

• Both PTVG and PRVG arrangements had significantly enhanced the heat transfer rate, in comparison to a smooth channel. The averaged heat transferred from surfaces with PTVGs was higher than that of the PRVGs. The disturbance in the boundary layer was formed due to punched holes, which created higher turbulence due to the separated and reattached flows.

• The present results reasonably agree well within the ±11.8% deviation for both the friction factor and Nusselt number correlations.

ACKNOWLEDGMENTS

The present work is financially supported by Hitit University (Grant No.MUH19003.14.001).

SYMBOLS

A	convection heat transfer area of channel (m^2)
D_h	hydraulic diameter (m)
f	friction factor (-)
e	height of winglet (m)
H	channel height (m)
h	averaged heat transfer coefficient (W/m^2 K)
k	thermal conductivity of air (W/m K)
Nu	Nusselt number (-)
Nu_{avg}	averaged Nusselt number (-)
S	spacing between longitudinal winglet (m)
ΔP	pressure drop (Pa)
Pr	Prandtl number (-)
PTVGs	punched triangular vortex generators
PRVGs	punched rectangular vortex generators
Re	Reynolds number (-)
Q	heat transfer (W)
T	temperature (K)
W	width of channel (m)
U	mean velocity (m/s)

Greek symbols

ε	Emissivity
σ	Stefan-Boltzmann-constant (W/m^2K^4)
α	attack angle of punched winglet (°)
ν	kinematic viscosity (m^2/s)

Subscripts

avg	average
0	channel without vortex generator

REFERENCES

[1] S. Tigglebeck, N.K. Mitra, M. Fiebig, Comparison of winglet type vortex generators for heat transfer enhancement in channel flow, ASME J. Heat Transfer 116 (4) (1994) 880–885.

[2] G. Biswas, K. Torii, D. Fujii, K. Nishino, Numerical and experimental determination of flow structure and heat transfer effects of longitudinal vortices in a channel flow, Int. J. Heat Mass Transfer 39 (16) (1996) 3441–3451 .

[3] M. Fiebig, P. Kallweit, N.K. Mitra, Winglet type vortex generators for heat transfer enhancement, in: Proceedings of the Eighth International Heat Transfer Conference, vol. 6, 1986, pp. 2909–2913.

[4] M.C. Gentry, A.M. Jacobi, Heat transfer enhancement by delta-wing vortex generators on a flat plate: vortex interactions with the boundary layer, Exp. Therm. Fluid Sci. 14 (3) (1997) 231–242.

[5] M.C. Gentry, A.M. Jacobi, Heat transfer enhancement by delta-wing-generated tip vortices in flat-plate and developing channel flows, ASME J. Heat Transfer124 (6) (2002) 1158–1168.

[6] G. Zhou, Q. Ye, Experimental investigations of thermal and flow characteristics of curved trapezoidal winglet type vortex generators, Appl. Therm. Eng. 37 (2012) 241–248.

[7] A.P. Rallabandi, D.H. Rhee, Z. Gao, J.C. Han, Heat transfer enhancement in rectangular channels with axial ribs or porous foam under through flow and impinging jet conditions, Int. J. Heat Mass Transfer 53 (2010) 4663–4671 .

[8] L.P.B.M. Janssen, M.M.C.G. Warmoeskerken, Transport Phenomena-Data Companion, DUM, Delft, 2, 1991.

[9] D. Lytle, B.W. Webb, Air jet impingement heat transfer at low nozzle plate spacings, Int. J. Heat Mass Transfer 37 (1994) 1687–1697.

[10] S.J. Kline, F.A. McClintock, Describing uncertainties in single-sample experiments, Mech. Eng. 73 (1953) 3–8.

[11] F. Incropera, P.D. Dewitt, Introduction to Heat Transfer, third ed., John Wiley &Sons Inc, 1996.